Available online at www.sciencedirect.com
SCIENCE DIRECT®
Journal of Power Sources 141 (2005) 108–115
JOURNAL OF POWER SOURCES
www.elsevier.com/locate/jpowsour

Development of a lightweight fuel cell vehicle☆

J.J. Hwang*, D.Y. Wang, N.C. Shih

Research Center for Advanced Science and Technology, Mingdao University, Peetou, Changhua 52345, Taiwan

Received 10 August 2004; accepted 30 August 2004
Available online 18 November 2004

Abstract

This paper described the development of a fuel cell system and its integration into the lightweight vehicle known as the Mingdao hydrogen vehicle (MHV). The fuel cell system consists of a 5-kW proton exchange membrane fuel cell (PEMFC), a microcontroller and other supported components like a compressed hydrogen cylinder, blower, solenoid valve, pressure regulator, water pump, heat exchanger and sensors. The fuel cell not only propels the vehicle but also powers the supporting components. The MHV performs satisfactorily over a hundred-kilometer drive thus validating the concept of a fuel cell powered zero-emission vehicle. Measurements further show that the fuel cell system has an efficiency of over 30% at the power consumption for vehicle cruise, which is higher than that of a typical internal combustion engine. Tests to improve performance such as speed enhancement, acceleration and fuel efficiency will be conducted in the future work. Such tests will consist of hybridizing with a battery pack.

Keywords: PEMFC; Vehicle; MHV

1. Introduction

In order to meet future transportation needs, most major car makers in the world actively are engaged in developing prototype fuel cell vehicles [1]. Fuel cell vehicles not only hold the promise of reduced urban pollution but also decrease the vehicles' dependence on petroleum. Hydrogen fuel cell vehicles are also key factors in the hydrogen economy—an economy with a vision of clean and sustainable energy for people's future power. Underlying such projected benefits is its fuel flexibility and higher efficiency compared to conventional gasoline-fueled internal combustion engines (ICEs).

In this paper, the results obtained from the development of the neighborhood fuel cell vehicle in Mingdao University is presented and discussed. Such development began in the year 2000 where an R&D activity on the fuel cell research was initiated. In the first phase of the fuel cell project, a 300 W fuel cell electric bicycle was successfully developed [2]. This paper describes the second phase of the project, which developed a fuel cell lightweight vehicle known as the Mingdao hydrogen vehicle (MHV). The major tasks included the design, the fabrication, the test and the demonstration of the prototype fuel cell electric vehicle.

MHV is a preliminary prototype fuel cell vehicle which does not optimize weight, dimension and configuration. The components chosen for the MHV should be commercially available. The availability and performance of each component and subsystem must also be tested independently. Then, a 5-kW PEM fuel cell system serving as the vehicle propulsion was built. After integrating the fuel cell system into the MHV, a series of tests were conducted in order to determine the performance of the MHV. Finally, driving tests and demonstrations were conducted after the necessary modifications.

The prototype also aimed to make the technology more acceptable in the market and to accelerate the national licensing process in this field of interest. The ultimate goal is to bring fuel cell technology out of the laboratory and into the marketplace. Such technology is seen to be of great significance in transportation as well as in power generation.

☆ An invited paper.

* Corresponding author. Tel.: +886 4887 6660; fax: +886 4887 9050.
E-mail address: azaijj@mdu.edu.tw (J.J. Hwang).

0378-7753/$ – see front matter © 2004 Elsevier B.V. All rights reserved.
doi:10.1016/j.jpowsour.2004.08.056

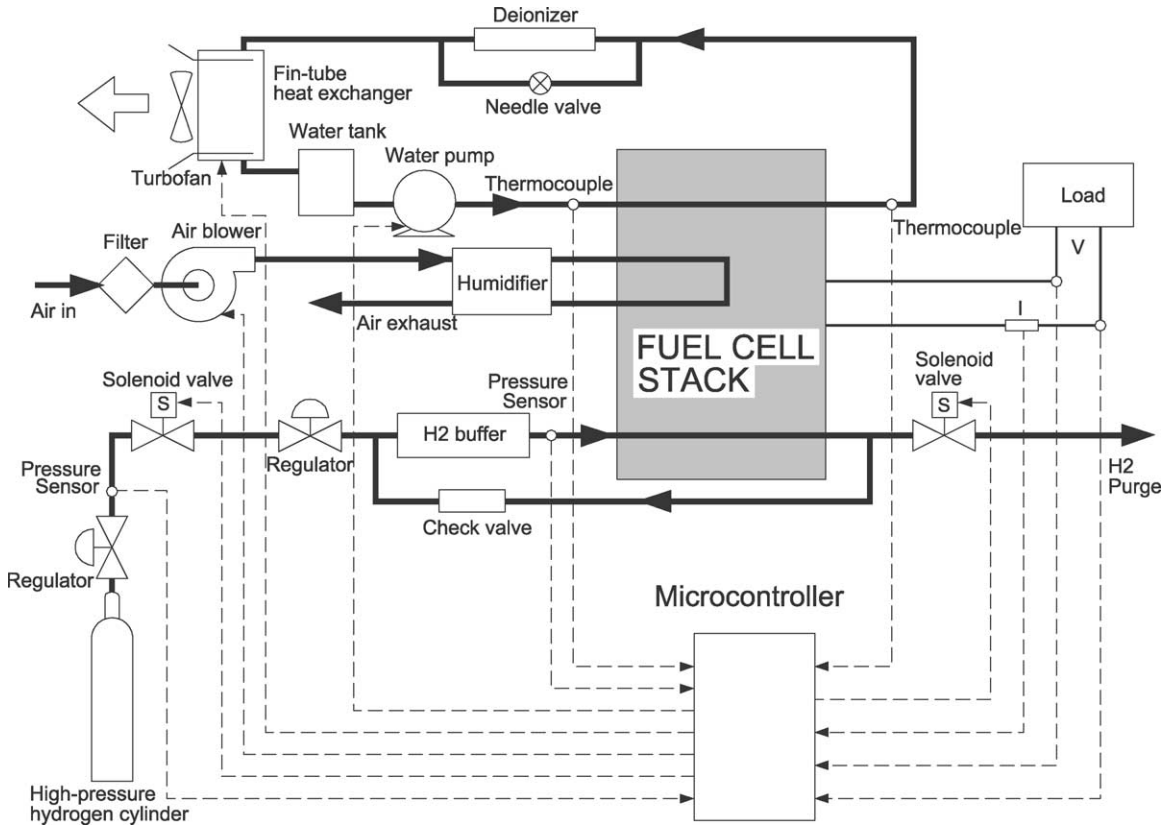

Fig. 1. Functional block diagram of the fuel cell system.

2. Fuel cell system design

The fuel cell stack is the heart of the fuel cell system; it cannot work without other support components. Therefore, the success in integrating a fuel cell system relies on the proper operation of each component in the system. Fig. 1 shows a functional block diagram of the present fuel cell system. The support components of the fuel cell system include a high pressure gaseous hydrogen cylinder, an air blower, a humidifier, solenoid valves, pressure regulators, sensors (temperature, pressure, voltage and current), a radiator, pipes and fittings. They are grouped into four subsystems and will be discussed in detail in the following sub-section, respectively, i.e. hydrogen fueling subsystem, air supply subsystem, cooling subsystem, and microcontroller. In general, subsystems are tied to each other. The design and construction of these subsystems are based on the fuel cell operating conditions listed in Table 1.

It is noted that fuel cells become contaminated if any of the components in the air supply subsystem, water cooling subsystem or hydrogen fueling systems are made of anything other than an inert substance like stainless steel, titanium, or certain grades of rubber or Teflon. Such requirements means dictates that many of the components have to be carefully selected, custom-built or ordered from laboratory supply companies. This is because most commonly available components are mild steel or low-grade rubber.

2.1. Fuel cell stack

Table 1 shows the specifications of the fuel cell stack (Asia-Pacific Fuel Cell Technologies Ltd.) utilized in the MHV. The stack consists of 70 cells with an active area of 150 cm^2. The nominal and peak powers are 3.2 kW (0.7 V) and 5.0 kW (0.6 V), respectively. The polarization curve shown in Fig. 2 is determined via a commercial test stand

Table 1
Characteristic data of the fuel cell stack

Specification	
Number of cells	70
Nominal power (at 0.7 V/cell)	3.2 kW
Nominal voltage	48 V
Nominal current	68 A
Peak power (at 0.6 V/cell)	5.0 kW
Active area	150 cm^2
Operation conditions	
Anode (pure H_2)	
Pressure	40 kPa
Temperature	70 °C
Relatively humidity	100%
Cathode (air)	
Pressure	40 kPa
Temperature	70 °C
Relatively humidity	100%
Stoichiometric ratio	2.5

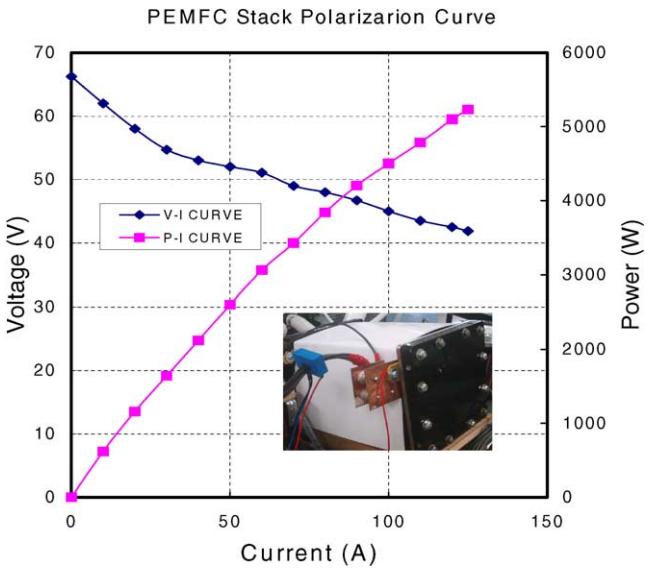

Fig. 2. Polarization curve of the PEMFC stack.

that can easily provide optimal operation conditions (such as temperature, pressure, humidity, etc.) for the stack [3]. It does not mean, however, that this fuel cell stack will follow this optimal curve during the real operation of the MHV. This is because the real drive conditions cannot be controlled optimally and precisely like those in the test stand.

The fuel cell stack not only provides the propulsion for the electric vehicle but also powers the components of all subsystems like the water pump. The drive motor can operate under a wide range of voltages (38–56 V). Thus, it is directly powered by the fuel cell stack of a large dynamic voltage. The electric power supplied to the supported components from the fuel cell stack should be regulated in voltages using dc/dc converters (Table 2).

2.2. Hydrogen fueling subsystem

The fuel cell uses pure hydrogen (>99.99%) as fuel. The hydrogen fueling subsystem is designed to store gaseous hydrogen in a cylinder at a moderate pressure of 20 MPa. This method is simple in design but the technology is well advanced. The pressurized hydrogen from the storage cylinder is passively reduced using manual regulators before entering the fuel cell stack. Thus, no additional energy is required as the hydrogen flows into the fuel feeding line.

As shown in Fig. 3, pure H_2 from the high-pressure gaseous hydrogen cylinder flows into the fuel management subsystem and enters the stack. Then, it returns back to the subsystem from the stack anode exit and either re-circulates into the H_2 buffer or is purged out. The pressure regulator reduces the pressure to the system pressure (~40 kPa). The pre-regulated pressure is measured and provided for the microcontroller in order to check on the remaining fuel stores. The signal from the post-regulated pressure sensor feeds into the microcontroller in order to ensure proper system pressure. A normal-closed solenoid valve ahead of the H_2 buffer turns on as the system pressure reduces to a predetermined value (e.g., <20 kPa). Such reduction is due to the electrochemical reaction. At the anode exit, a passive hydrogen recirculation is implemented in the fuel management subsystem by incorporating a check valve between the stack outlet and the H_2 buffer inlet. Hydrogen recirculation is imperative in order to maximize the fuel usage and system efficiency. As shown in Figs. 1 and 3, the bypass of the anode exhaust is equipped with another solenoid valve to conditionally purge anode exhausts and inert as the stack voltage is reduced to a predetermined value (e.g., 44 V).

2.3. Air supply subsystem

The air supply subsystem provides the fuel cell stack with clean air of RH > 80% (relative humidity). As shown in Fig. 1, the ambient air is drawn into the oxidant feeding line and through a particular-designed filter using a motor-blower to keep it away from dusts or oils. A load-following technique is employed in the design of the oxidant supply subsystem, that is, the blower varies its flow rate in order to meet the requirement of oxidant for the electrochemical reaction. This can be achieved by changing the motor speed via a pulse width modulation control. The strategy of the cathodic oxidant supply in different power conditions is summarized as follows:

1. At low power consumption, the air flow rate is kept at a constant level that supports the electrochemical reaction.

Table 2
Typical power consumption or conversion efficiency of the components of the fuel cell power system

Components	Quantity	Electric specification[a]	Maximum power consumption	Conversion efficiency (%)
Motor I	1	48 V/9.5 A	4 kW	–
Motor II	1	12 V/0.8 A	10 W	–
Blower	1	24 V/10 A	250 W	–
Solenoid valves	2	12 V/0.12 A	2.8 W	–
Cooling fans	1	12 V/0.15 A	7.2 W	–
Water pump	1	24 V/0.8 A	20 W	–
Microcontroller	1	12 V/2 A	24 W	–
Converter I	1	48–24 Vdc	–	90
Converter II	1	48–12 Vdc	–	90

[a] Data from manufactures.

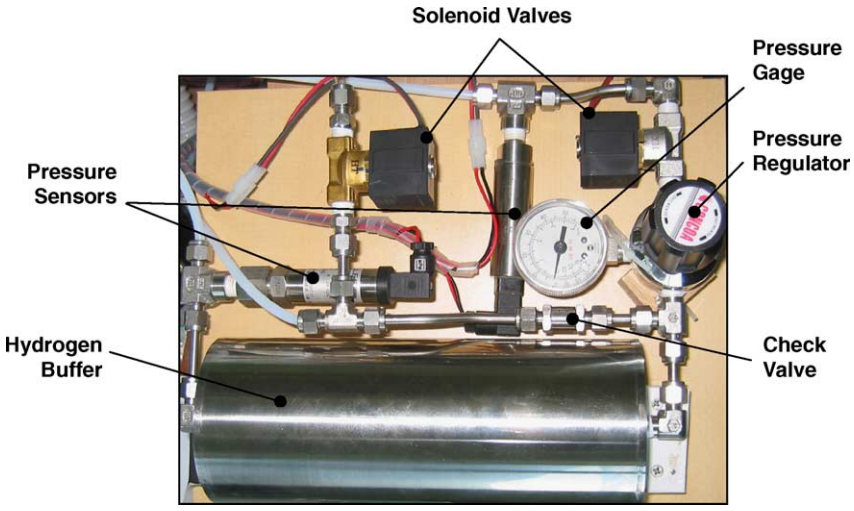

Fig. 3. Fuel management subsystem.

2. At high power consumption, the air flow varies in order to meet the manufacturer's recommended stoichiometric ratio of 2.5 (Table 1), that is, as the power delivery by the fuel cell increases, the blower motor speed increases in order to provide more oxidant to the cathode. This is because the stoichiometric ratio is less than 2.5. Conversely, the blower motor slows down as the fuel cell power is reduced. Such an action benefits the system efficiency through power saving.
3. As the fuel cell system starts or resets, the blower runs with full power in a short period in order to remove the water and/or inert inside the cathode.

In the above mentioned conditions, the stoichiometric ratio of the cathode oxidant is always larger than 2.5. The purpose of the high oxidant stoichiometric ratio in the stack cathode is not only the supply of enough oxygen to the cathode but also the effective removal of the by-product water from the cathode using a strong cathode stream [4].

Reactant humidification is critical to the performance of a PEM fuel cell stack particularly the oxidant. In the present work, an enthalpy-wheel humidifier is employed to humidify the cathodic inlet oxidant. As shown in Fig. 1, warm and humid air exiting from the stack cathode enters the humidifier. A rotating drum absorbs the exhaust water vapor and transfers it to the incoming cool and dry air stream. The characteristics of the desiccant-coated drum allow only the water vapor to be transferred. The spent gases exit the humidifier. The water vapor never condenses thus, requiring no external energy to move it back into vapor form.

2.4. Cooling subsystem

The fuel cell stack is water-cooled. As shown in Figs. 1 and 4, the cooling subsystem consists of a water pump, a deionizer, a water tank, two thermocouples and a fin-tube heat exchanger together with a turbofan. Cooled water from the reservoir is pumped into the stack by a water pump. The water pump is a combination of a dc-24 V motor with magnetic-drive seal-less head and ceramic impellers. Hot water exiting from the stack outlet passes through a deionizer and is then drawn into the fin-tube heat exchanger. The deionizer is similar in shape, size and function to the household water purification systems. The fin-tube heat exchanger is made of 316 stainless welded steel tubings with copper fins and a low-profile turbofan in a 'push' configuration. Two thermocouples are located at the stack inlet and outlet, respectively. The thermocouples measure the temperature rise across the fuel cell stack and determine the removed heat from the stack using the radiator. In addition, the turbofan is triggered by the microcontroller depending on the change in the stack outlet (water) temperature. As shown in Fig. 5, when the temperature is higher than $T > 45\,^{\circ}C$, the turbofan is turned on in order to remove the heat that is produced by the electrochemical reaction. When the stack outlet temperature is decreased and is lower than 40 °C, the turbofan is switched off for power saving purposes. When the fuel cell system is reset or shutdown, the turbofan together with the water pump is kept 'on' immediately (e.g., 20 s).

2.5. Microcontroller

Controlling the fuel cell operation requires a smart microcontroller together with the proper algorithm that safely starts, monitors and shuts down the fuel cell under all operating conditions. In the present fuel cell system, an Intel 8051 microprocessor acts as the head of the system. As shown in Fig. 1, the microcontroller is capable of monitoring the sensor signals of voltage, current, temperature, and pressure. It also takes appropriate actions in order to drive the external devices such as the air blower, the solenoid valve, the water pump and the turbo-fan. A remote LCD display located on the vehicle board is interfaced with the microcontroller in order to monitor the output of the system. In addition, the

Fig. 4. Cooling subsystem of the fuel cell system (water pump is behind the heat exchanger).

voltage of each cell within the fuel cell stack is monitored in a 70-channel analog multiplexer in order to detect individual cell failures early. Custom-built analog isolation amplifier circuits are used to isolate the microcontroller from the fuel cell stack's high voltage output. In the event of a shutdown, the microcontroller stores the current system parameters. These parameters can be read directly from the LCD display or can be downloaded to the personal computer through the RS232 communication port on the microcontroller.

3. Vehicle body and transmission system

In the present work, an existing vehicle body and a commercial transmission system are used to construct the body and the drivetrain of the MHV. The vehicle body was rebuilt from a battery-based electric vehicle that originates from the Tang Eng Iron Works Co. Ltd. In general, the overall integrity of the vehicle body is good. Most of the functions such as the lighting, the parking break and the steering remain intact. The majority of change lies in remodeling the rear seats into the space for the fuel cell engine (Fig. 6). A continuous variable transmission system (Yi-Jan Electric Motion Enterprise) is employed in the fuel cell electric vehicle. A 4-kW/48 V dc motor is mounted directly on the transmission. The motor comes with a flexible coupling installed on the input shaft. The transmission has a fully synchronized variable speed trans-axle combined with a ratio selection and a differential function in one unit housed in a die-cast aluminum case. A motor controller is used for both commutation and control functions. Such controller is capable of driving the motor both forward and reverse with analog inputs from −10 V (full reverse) to 10 V (full forward). Therefore, a reversing gear, although available, is not required. The motor can deliver a constant torque of 23 kgm from 2800 rpm. The maximum speed is 4000 rpm and the maximum efficiency is 96%. A hall-effect sensor in the motor is used for determining the timing information needed for motor commutation. These signals are processed by the controller and compared with the desired speed. In the event that the controller or motor overheats, the controller will automatically limit the current by itself.

The curb weight of the vehicle body along with the transmission system is approximately 800 kg, including the fuel cell system.

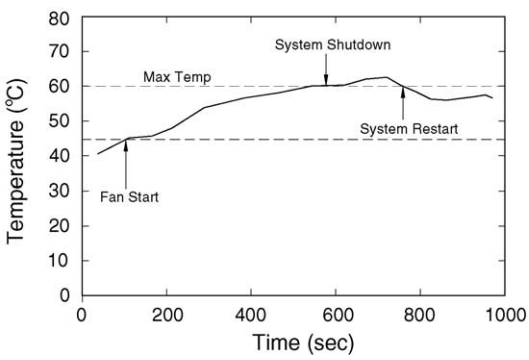

Fig. 5. Typical cooling strategy of the fuel cell system.

Fig. 6. Installation of fuel cell system on the rear seat of the electric vehicle.

4. Results and discussion

4.1. System efficiency

Before integrating the fuel cell system, each sensor is calibrated using a laboratory-quality instrument that ensures its accuracy (with uncertainties less than 5%) and reliability over the ranges in which it is operated. In the meantime, each actuator such as the solenoid valve and the relay is tested independently in order to check its availability and performance. These supported components are then installed on the fuel cell system. A series of static tests in the laboratory is conducted in order to determine the efficiency of the fuel cell system.

The efficiency of the fuel cell system is determined by accounting for the generation efficiency of the fuel cell stack, the efficiency of the power conversion devices and the load of the power-consumed components. Table 2 lists the electric features of the supported components in the fuel cell system provided by the manufactures. The present work, however, does not use such an approach since it is difficult to accurately determine the efficiency of each power conversion device and the power consumption of the supported accessory. For example, it is hard to catch the real power dissipation by the load-following blower, which fluctuates by the speed-up and the slow-down of the motor during the operation. The system efficiency is herein defined as the ratio of the net power delivered to the drive motor from the fuel cell to the enthalpy flow of the consumed hydrogen, i.e.,

$$\varepsilon = \frac{I \times V}{\dot{n} \times \Delta h} \tag{1}$$

The numerator of the above equation represents the net power for the vehicle propulsion measured directly, the voltage (V) across the drive motor and the current (I) passing through the circuit. The mole flow rate of hydrogen delivered from the cylinder to the fuel cell system in the test duration (Δt) is

$$\dot{n} = \frac{1}{RT}\frac{P_{\text{initial}} - P_{\text{final}}}{\Delta t} \tag{2}$$

P_{initial} and P_{final} are the compressed hydrogen cylinder pressures at the initial and final conditions, respectively. They are read from the pressure sensors.

Fig. 7 shows the efficiency of the fuel cell system as a function of the gross power output of the fuel cell stack. These system efficiency data are based on static-load testing, which is a good representation of how the fuel cell system performs over a variety of loads. The general trend of the system efficiency is an increase with increasing gross power output which compares well to test results from other researches made on fuel cell systems [5]. Concerning the power required for cruise speed, the system efficiency must be above 30%, which is higher than that of an ICE. Despite this, there is much room for improvement during the first attempt to build a fuel cell system for the propulsion of an electric vehicle in the laboratory.

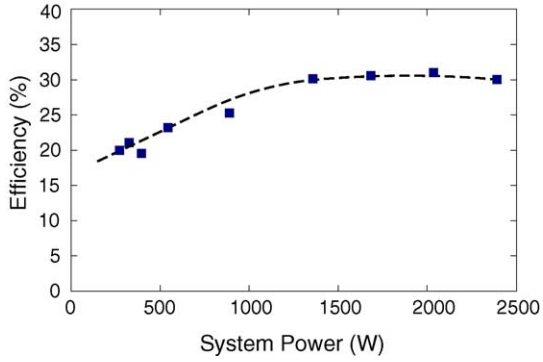

Fig. 7. System efficiency of the fuel cell electric vehicle.

After installing the fuel cell system on the MHV and finishing the needed modifications, road-driving tests must be conducted. The road test of the MHV is done via a 1.6 km-run inside the Mingdao campus, as shown in Fig. 8. The speed of the MHV is kept at about 18 km h^{-1}. The road test reveals that the MHV displays reliable operation without any failure during the one-hour test. This indicates that the stability and reliability of the present system are, to a certain extent, satisfactory. The specifications of the MHV are summarized in Table 3. Up to the present time, the MHV has successfully completed the drive over a 100 km run. The maximum speed shown in Table 3 is estimated by the maximum power of the propulsive motor, the vehicle weight, the drag and the rolling resistance rather than the power delivery by the fuel cell power.

4.2. Safety and reliability

The safety of hydrogen-powered vehicles is usually a matter of concern. During the assembly and testing of the MHV, no accidents, hazardous or potentially hazardous situations were experienced. Before each run, regular leakage checks

Fig. 8. Driving test of MHV in the Mingdao campus.

Table 3
Features of the MHV

Vehicle	Dimensions, L/W/H	3120/1350/2030 mm
	Weight	800 kg
	Maximum load capacity	400 kg
Performance	Average cruising speed	18 km h^{-1}
	Electric power required for cruising speed	2 kW
	Maximum speed	40 km h^{-1}
	Start-up/Shut-off time	10/20 s
	Emission	Pure H_2O
	Noise	80 dB at 1 m
	Safety	No accidents or any hazardous situations
Drive	Type	Rear motor, rear wheel drive
Drive motor	Type	dc 48 V, permanent-magnet synchronous
	Maximum power	4.0 kW
	Maximum torque	23 kgm/2800 rpm
Transmission	Differential ratio	1:22
	Distance between 2 wheels	950 mm
	Others	Drum brake inclusive
Fuel cell	Type	PEM
	Rate power/voltage	3.2 kW/0.7 V/cell
Hydrogen storage device	Type	High pressure gaseous hydrogen cylinders
	Dimensions, diameter/height	150/670 mm
	Hydrogen storage capacity	1400 L

were conducted for the entire hydrogen feeding line such as the pipes, the fittings, the valves and the fuel cell stack. The microcontroller automatically performs a shutdown whenever it detects a parameter out of a prescribed range. During the test drives, intermittent shutdowns were experienced. The main causes of these shutdowns are overheating of the propulsive electric motor, fuel cell problems indicated by low voltage and depletion of hydrogen.


總統搭燃料電池車遊園

〔記者周為政員林報導〕師生努力提升台灣科技。台灣花博會開幕，陳水扁總統特地搭乘由明道學院校長駕駛的氫能源的燃料電池車為全台第一部，更首創由大學獨立研發的創遊園，陳總統稱許明道學院。

。園遊車池電料燃的源能氫坐乘統總扁水陳

（攝政為周者記）

Fig. 9. An episode of the demonstration of MHV in “2004 Taiwan Flower Exposition”, reported by Taiwan Times (President Chen Shui-Bian, the second one from the right).

4.3. Demonstration

Fig. 9 shows an episode of the demonstration of MHV in the “2004 Taiwan Flower Exposition” (from January 17 to March 14, 2004), which was reported by Taiwan Times.[1] President Chen Shui-Bian was one of the riders in the demonstration. In this report, President Chen not only celebrated the opening of the Exposition but also deeply praised Mingdao University for the successful development of the first fuel cell vehicle in Taiwan. It is believed that the above demonstration has verified the viability of the fuel cell technology and is a significant development in Taiwan.

5. Conclusions

Phase II of the Mingdao fuel cell project has been completed after successfully finishing the development of the lightweight fuel cell vehicle known as the MHV. Informative outcomes and experiences obtained from the design, fabrication and testing of this prototype will be helpful in future studies on the fuel cell technology. By comparing the results obtained to the first phase, several differences and advantages in the present work are:

1. Cathode humidification is applied to the present air supply subsystem. Such a process was not considered in developing the low-power fuel cell bicycle.

[1] A nationwide newspaper in Taiwan.

2. Hydrogen recirculation is implemented in the present fuel management subsystem in order to enhance the fuel usage. This was not considered in the previous work.
3. A water-cooled scheme is employed in the present 5-kW fuel cell system while the previous 300-W fuel cell was cooled by ambient air.
4. A load-following technology has been used in the MHV in contrast to the oxidant supply used by two constant-speed air pumps.

The next stage of the project will focus on the hybrid system, i.e., combining the battery in the fuel cell electric vehicle. The power demands of a hybrid vehicle are dependent not only on the fuel cell but also on the battery pack. In addition, hybrid vehicles generally have the capability of regenerative energy storage [6]. Optimizing the degree of hybridization (size of battery versus size of fuel cell) will be the center of attention in future endeavors.

Acknowledgement

This work was partly sponsored by National Science Council of Taiwan under contract no. NSC 93-2212-E451-002.

References

[1] Fuel cell vehicle world survey 2003. Breakthrough Technologies Institute, Washington, D.C, 2004.
[2] J.J. Hwang, D.Y. Wang, N.C. Shih, D.Y. Lai, C.K. Chen, J. Power Sources 133 (2004) 223–228.
[3] J.J. Hwang, H.S. Hwang, J. Power Sources 104 (2002) 24–32.
[4] J.J. Hwang, C.K. Chen, R.F. Savinell, C.C. Liu, J. Wainright, J. App. Electrochem. 34 (2004) 217–224.
[5] D.J. Frdman, R.M. Moe, PEM Fuel Cell System Optimization, in: Second International Symposium on Proton Conducting Membrane Fuel Cells, The Electrochemical Society Inc., Pennington, NJ, 1998.
[6] K. Morita, JSAE Rev. 24 (2003) 3–7.